VOICE AND GESTURE BASED WHEELCHAIR CONTROLLER FOR PHYSICALLY HANDICAPPED

E.Sowmiya,K.Vanmathi,T.Ramya, UG Scholar Department Of ECE, Nandha College Of Technology,
Mrs.T.Padmavathi, Assistant Professor, Department Of ECE,Nandha College Of Technology,

ABSTRACT

Wheelchairs are used by the people who cannot walk due to physical illness, injury or other disability. Now a day's development promises a wide scope in developing smart wheelchair. This paper is to describe an intelligent wheelchair using smart phone is to develop to control the rotation of wheelchair based upon voice and gesture movement for the physically challenged persons. In build voice and gesture function are used to control the wheelchair as well as by using smart phones reading SMS, E-mail, and News. In this system Thermostat is used to monitor the Body temperature and heart beat. This system that allows the user to robustly interact with the wheelchair at different levels of the control and sensing .The system is divided into 3 main units Voice recognition, gesture recognition and Motor control through signal conditioning. The system is based on grouping an Android phone with Microcontroller.

Index Terms—Android phone, Microcontroller PIC16F877A, Gesture recognition, Thermostat, HC-05 Bluetooth module.

1. INTRODUCTION

Overall, worldwide about 100 million to 130 million people need wheelchairs. Wheelchairs are a source of mobility for them and essential to their daily lives. It feels they are in danger. Some people also insist on using manual wheelchairs for the exercise.

Unfortunately day by day the number of handicapped people is increasing due to road accidents and diseases like paralysis. Among all the disabilities the percentage of physically handicapped people is most. If a person is Handicapped is dependent on other person for his day work like transparent, food and Orientatation.

The aim of this project is to use wheelchair automatically and operate by using voice and gesture control for moving forward, backward, left and right by using Bluetooth and Android. Quadriplegics and multiple sclerosis patients have severe disabilities and cannot drive joystick operating traditional wheelchairs.

A manual wheelchair is propelled by the force of the arms, and it has little difficulty moving back and forth on a flat road, but propulsion up a hill is a great challenge to the wheelchair rider. An electric wheelchair, driven by electric motors and controlled by a joystick, can move anywhere with ease, but it is too heavy and large to be loaded into a regular car. Moreover, it can't perform complicated maneuvers in a narrow or confined space, such as in offices or homes, such that the people around switches driving mode into an electric mode on a hill and turns the with more than the threshold torque.

A wheelchair is fitted with DC motor, GSM, Bluetooth, Thermostat, IR sensor and Smartphone. By just tilting smart phone which is with the wheelchair user wheelchair can be moved in four directions. The approach allows the user to use Human voice, Gesture movement Smartphone and synchronize with the movement of wheelchair so that they can use it with comfort.

The complexity is reduced by using Smartphone so that the size of the system is very compact.

2. ANDROID

Android is a software stack for mobile devices that includes an operating system,

middleware and key applications. The Android SDK provides the tools and APIs necessary to begin developing applications on the Android platform using the Java programming language

3. HARDWARE DESCRIPTION

The components used in this project are Microcontroller PIC 16f877a, DC motor, motor driver, GSM, Thermostat , Bluetooth, Android, smart phone and battery source.

3.1 BATTERY SOURCE

These are also sometimes called Primary Cells. Inside are two electrodes. One is made of Zinc and the other is made of Manganese Oxide. These make up the positive and negative terminals respectively. The electrodes are surrounded by an alkaline electrolyte, hence their name. Basically what happens inside is the electrolyte causes electrons to move from the zinc electrode to the manganese oxide electrode. This transfer of electrons causes a current to flow. The zinc and Manganese have a resistance, which cause a voltage to develop across them both due to the current passing between them. This voltage is 1.5V. Now, unfortunately this chemical reaction does not go on forever. Eventually, the electrolyte will be weakened and there will be no more voltage at the electrodes. This is when we decide to throw the battery away.

3.2 THERMISTORS

Thermostats are temperature sensitive resistors. All resistors vary with temperature, but thermostats are constructed of semiconductor material with resistivity that is especially sensitive temperature. However unlike most other resistive devices the resistance of a thermostat decreases with increasing temperature. That is due to properties of the semiconductor that the resistor is made from Thermostats are expensive, easily-obtainable temperature sensor. In this system the thermostat is fitted to detect and monitor the body temperature of handicapped persons. They are easy to use and adaptable.

3.3 BLUETOOTH

Bluetooth is wireless technology standard for exchanging data over short distances using short – wavelength UHF radio waves in the ISM band from 2.4 to 2.485 GHZ from fixed and mobile devices and building personal area networks (PANs). A Bluetooth device uses radio waves instead of wires or cables to connect to a phone or computer. A Bluetooth product like a headset or a watch contains a tiny computer chip with a Bluetooth radio and software that makes it easy to connect.

Bluetooth is managed by the (SIG) which has more than 30,000 member companies in the areas of telecommunication, computing, networking, and consumer electronics. The IEEE standardized Bluetooth as **IEEE 802.15.1**, but no longer maintains the standard. The Bluetooth SIG oversees development of the specification, manages the qualification program, and protects the trademarks. A manufacturer must meet Bluetooth SIG standards to market it as a Bluetooth device. Networks of patents apply to the technology, which are licensed to individual qualifying devices. Invented by telecom vendor Ericsson in 1994, it was originally conceived as a wireless alternative to RS-232 data cables. It can connect up to seven devices, overcoming problems that older technologies had when attempting to connect.

3.4 GSM (GLOBAL SYSTEM FOR MOBILE COMMUNICATION)

A GSM modem exposes an interface that allows applications such as SMS to send and receive over the modem interface. The mobile operator charges for this message sending and receiving as if it was performed directly on a mobile phone. To perform these tasks a HSM modem must support an "Extended AT command set for sending/receiving SMS messages. **GSM** (**Global System for Mobile Communications**, originally ***GroupeSpécialMobile***) is a standard developed by the European Telecommunications Standards Institute (ETSI) to describe the protocols for second-generation (2G) digital cellular networks used by mobile phones, first deployed in Finland in July 1991. As of 2014 it has become the de facto global standard for mobile communications – with over 90% market share, operating in over 219 countries and territories. 2G networks developed as a replacement for first generation (1G) analog cellular networks, and the GSM standard originally described as a digital, circuit-switched network optimized for full duplex voice telephony. This expanded over time to include data communications, first by circuit-switched transport, then by packet data transport via GPRS (General

Packet Radio Services) and EDGE (Enhanced Data rates for GSM Evolution or EGPRS).

3.5 DC MOTOR

A DC motor in simple words is a device that converts direct current into mechanical energy. It is of vital importance for the Industry today and it is equally important for engineers to look into the Working principle of DC motor. The very basic construction of DC contains a current carrying armature which is connected to the supply end through commutate segments and brushes it is placed within the north south poles of a permanent or an electromagnet.

3.6 MICROCONTROLLER PIC 16f877a

A **microcontroller** (or **MCU** for *microcontroller unit*) is a small computer on a single integrated circuit. In modern terminology, it is a System on a chip or Sock A microcontroller contains one or more CPUs (processor cores) along with memory and programmable input/output peripherals. Program memory in the form of Ferroelectric RAM, NOR flash or OTP ROM is also often included on chip, as well as a small amount of RAM. Microcontrollers are designed for embedded applications, in contrast to the microprocessors used in personal computers or other general purpose applications consisting of various discrete chips Microcontrollers are used in automatically controlled products and devices, such as automobile engine control systems, implantable medical devices, remote controls, office machines, appliances, power tools, toys and other embedded systems. Or microwatts).

3.6 IR SENSOR

An infrared sensor is an electronic device that emits in order to sense some aspects of the surroundings. An IR sensor can measure the heat of an object as well as detects the motion. These types of sensors measures only infrared radiation, rather than emitting it that is called as a passive IR sensor. Usually in the infrared spectrum, all the objects radiate some form of thermal radiations. These types of radiations are invisible to our eyes that can be detected by an infrared sensor. The emitter is simply an IR LED (Light Emitting Diode) and the detector is simply an IR photodiode which is sensitive to IR light of the same wavelength as that emitted by the IR LED. When IR light falls on the photodiode, the resistances and these output voltages, change in proportion to the magnitude of the IR light received.

3.7 PHOTO DIODE

A **photodiode** is a semiconductor device that converts light into current. The current is generated when photons are absorbed in the photodiode. A small amount of current is also produced when no light is present. Photodiodes may contain optical filters, built-in lenses, and may have large or small surface areas. Photodiodes usually have a slower response time Photodiodes are similar to regular semiconductor diodes except that they may be either exposed (to detect vacuum UV or X-rays) or packaged with a window or optical fiber connection to allow light to reach the sensitive part of the device. Many diodes designed for use specifically as a photodiode use a PIN junction rather than a p–n junction, to increase the speed of response. A photodiode is designed to operate in reverse bias as their surface area increases. The common, traditional solar cell used to generate electric solar power is a large area photodiode. A motor driver IC is an integrated circuit chip which is usually used to control motors in autonomous robots. Motor driver ICs act as an interface between microprocessors in robots and the motors in the robot. The most commonly used motor driver IC's are from the L293 series such as L293D, L293NE, etc. These ICs are designed to control 2 DC motors simultaneously. L293D consist of two H-bridge. H-bridge is the simplest circuit for controlling a low current rated motor

4. PLATFORM DESIGN

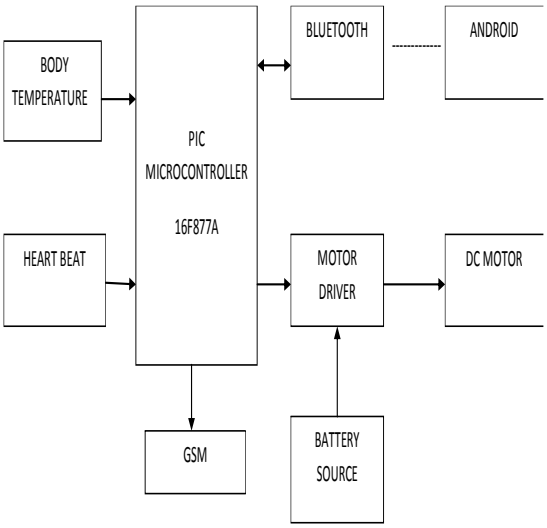

5. CONCLUSION

By using this system physically handicapped people easy way to navigate within the house using wheelchair without the external help. This provides is of operation as the system uses smart phone so that accuracy is increased.

The reading of SMS, E-mail, and News can be possible. The IR Sensor describes the parameter like heart beat and Thermostat monitors body temperature. The IR sensor is used for obstacle avoidance. If any emergency then the Panic button is there it blows buzzer.

REFERENCES

[1] R. Lu, Z. Li, C.-Y. Su, and A. Cue, "Development and Learning Control of a Human Limb with a Rehabilitation Exoskeleton," *IEEE Trans. Ind. Electron.*, vol. 61, no. 7, pp. 3776-3785, Jul. 2014.

[2] J. Zhu, Q. Wang, and L. Wang, "On the Design of a Powered Prosthesis with Stiffness Adaptable Ankle and Toe Joints," *IEEE Trans.* vol. 61, no. 9, pp. 4797-4807, Sep. 2014.

[3] R. J. Farris, H. A. Quintero, S. A. Murray, K. H. Ha, C. Harridan, and Goldfarb, "A Preliminary Assessment of Legged Mobility Provided by a Lower Limb Exoskeleton for Persons With Paraplegia," *IEEE Trans.*.

[4] Hirokazu Seki, K.Ishihara "Novel Regenerative Braking Control of Electric Power-Assisted Wheelchair for Safety Downhill Road Driving," *IEEE Trans. Ind. Electron.*, vol. 56, no. 5, pp.1393-1400, May 2009.

[5] Yamaha wheelchair assist unit, http://www.yamaha-motor.co.jp/wheelchair/lineup/jwx2/ (in Japanese).

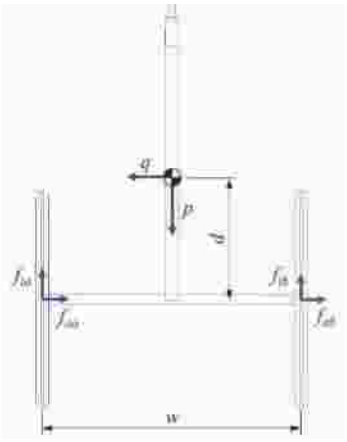

Fig. 6. Free body diagram of a wheelchair on a two-directional slope.

Fig. 6 shows the free body diagram on the sloping surface in Fig. 5. The force and moment equilibrium equations are (9) and (10).

$$f_{ta} + f_{tb} = mg = \frac{\text{weight of wheelchair}}{\text{acceleration of gravity}} \quad (9)$$

$$(f_{tb} - f_{ta})\frac{w}{2} = M_\gamma = \frac{\text{inertia moment of wheelchair}}{\text{angular acceleration}} \quad (10)$$

Then

$$f_{ta} = \frac{mg(\sin\theta - \mu\cos\theta)}{2} \quad (11)$$

=

$$0 \quad (12)$$

$$f_{tb} = \frac{mg(\sin\theta + \mu\cos\theta)}{2}. \quad (12)$$

The required right and left wheel torques for gravity compensation can be derived by multiplying the tangential forces f_{tb} and f_{ta} by the wheel radius, respectively. Therefore, if it is necessary, the wheelchair can precisely compensate for the gravitational force when the wheelchair ascends on a slant (the quantitative consideration is mentioned in section IV-E).

III. Prototype

To verify the effectiveness of the proposed compensating method, a prototype was designed. A lightweight folding commercial wheelchair (Miki Ltd., Mirage) was remodeled. Fig. 7 shows the system configuration of the prototype.

As a driving motor, a commercially available coreless motor was used to eliminate cogging torques that can cause unexpected vibrations when the rider rotates the pushrim. The energy consumption of the motor was considered since the wheelchair is battery-powered. A motor that consumes less energy when the wheelchair is paused on a hill was preferred. The relation between the power consumption in the stall condition and the parameters of the motor was investigated.

$$i = \frac{T}{k_t N} \quad (13)$$

Here, i is current applied to the motor when the wheelchair is

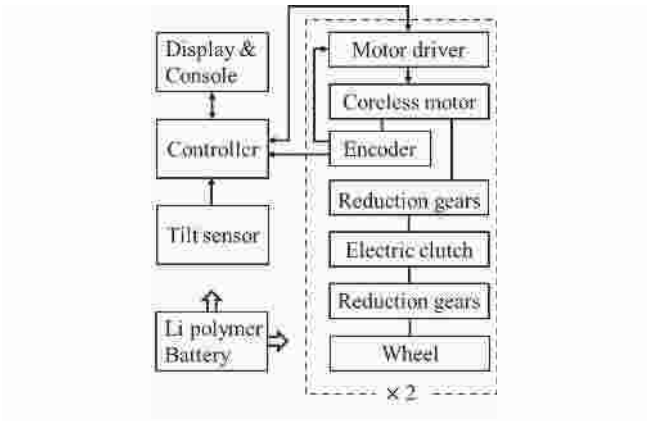

Fig. 7. System configuration of the prototype.

paused on a hill, T is torque applied to the wheel, k_t is torque constant, and N is the reduction ratio.

The heat dissipation P, is calculated from the current and terminal resistance.

$$P = \frac{\text{power}}{\text{time}} \cdot R = R i^2 \cdot \frac{\text{time}}{\text{motor}} \cdot \frac{1}{\text{motor}} \quad (14)$$

Here, R is terminal resistance of the motor.

In (14), $R i^2$ is irrelevant to the characteristics of the motor, and is determined by the mass of the wheelchair and the angle of the inclined plane. $\frac{\text{time}}{\text{motor}}$ generally decreases as the motor size increases. Therefore, although nominal output powers are the same, a bigger motor consumes less energy in stall condition, but a bigger motor increases the wheelchair weight. On the other hand, when nominal output powers are the same, generally a smaller motor has a higher nominal speed, and the reduction gear ratio becomes larger. In this regard the smaller motor is advantageous, but a smaller motor has a small heat capacity and the high speed rotation and high reduction gear ratio may cause noise.

In this research, the driving motor was selected by considering the heat conditions described above and the motor power required [26].

The following are the assumptions and conditions considered in selecting the motor for the GCPAW.

- Maximum output point: 5 km/h (fast walking speed) at a 6-degree angle
- Maximum weight: 120 kgf (wheelchair user's weight is 100 kgf, and the wheelchair's weight is 20 kgf)
- Efficiency of reduction gear set: 90%
- Rolling resistance: 1 % of vertical force
- Wheel diameter of GCPAW: 22 inches (559.8 mm)
- Inertia force (force required to accelerate or decelerate the GCPAW) is neglected

The required motor power P_w (power per one motor) to climb the slope of a 6-deree angle at the speed of 5 km/h is calculated as follows.

□ = ×

×

پ

(
1
5
)

ه

where f_r is the rolling resistance coefficient, η is the efficiency of the reduction gear set, and v is the wheelchair speed. When m = 120 kg, g = 9.8 m/s, θ = 6 deg, η = 0.9, f_r = 0.01, and v = 1.389 m/s (= 5 km/h), then P_w=103.9 W. A moving-coil type motor (Maxon RE40, 48 V), was selected because its nominal power is 150 W, and its coil resistance is low (1.16 ohm).

To determine the appropriate gear reduction ratio, the permitted torque-speed area of the motor and the required power (103.9 W) curve, with some reduction ratios, were drawn (Fig. 8). Commercially available reduction gears are usually heavy, and it was difficult to find the necessary reduction ratio and connecting conditions. Therefore, a customized reduction gear was developed, which is shown in Fig. 9. The reduction ratio was determined at 1000/7 (142.9), which was well within the continuous operation area, considering the number of teeth in the available gears and pulleys.

An electromagnetic clutch (Ogura, AMP-5) was installed among the reduction gears to connect or disconnect the wheel with the motor. Installing an electromagnetic clutch among gears has an advantage over installing it next to the output shaft or the input shaft. Installing it next to the output shaft can completely remove the effect of friction of the reduction gear when the rider turns the pushrim, but the clutch needs a larger capacity of torque transmission. Installing it next to the input shaft requires less torque transferring capacity, but it requires higher speed capacity. Therefore, the clutch was installed among the gears to maximally use the torque and speed capacity.

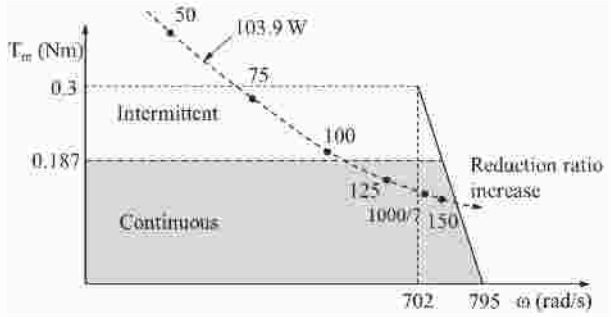

Fig. 8. Permitted torque-speed area of the drive motor and the required power curve with some reduction ratios.

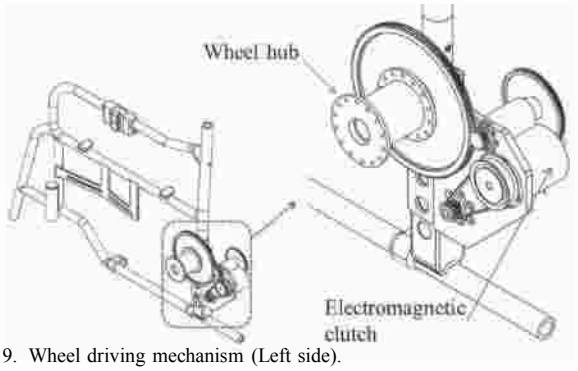

Fig. 9. Wheel driving mechanism (Left side).

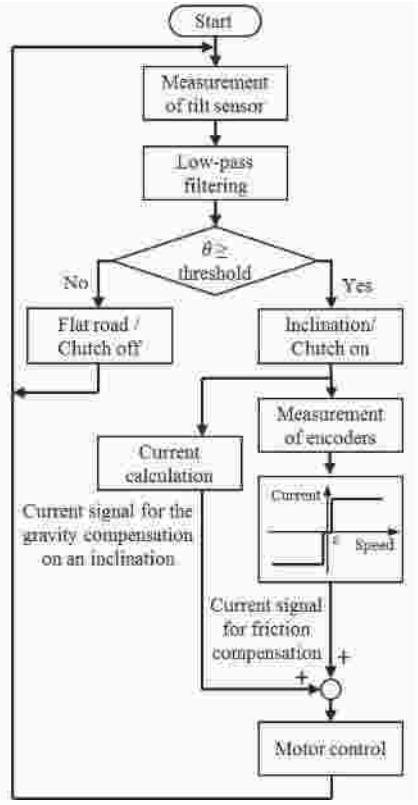

Fig. 10. Control algorithm for gravity and friction compensation.

The entire system was controlled by an MCU (STM320F103) board with a control cycle of 10 ms. The wheelchair included a tilt sensor (DAS, MSENS-IN-30) that measures the angle of the inclined plane and motor encoders to measure the rotating angle of the motor (1024 pulse/rev). Table 1 shows some specifications of the tilt sensor used in this research.

TABLE I
SOME SPECIFICATIONS OF THE TILT SENSOR

Description	Specs
Range	±30°
Resolution	0.1 deg
Nonlinearity	0.25% (FS)
Response time	< 0.08 s
Axis	2

The motors were controlled by a motor driver (Robocube, Cube BL4808- DID). The MCU board read the tilt sensor signal, calculated the necessary current and sent a current command to the motor driver. A lithium polymer battery was used as the power supply. Fig. 10 shows the control algorithm for gravity and friction compensation.

IV. EXPERIMENT

A. Measurement of Friction in the Driving Mechanism

The friction in the driving mechanism was measured as reference data for the friction compensation (in (2)). The

wheelchair was suspended. The wheel was rotated by an external driving device and the torque of the driving device was measured. Fig. 11 shows the results. The static friction was relatively large compared to the dynamic friction. The reason for this was assumed to be that the friction is not just the friction between two surfaces, but that it includes the friction between a lot of surfaces and resistance from the dynamic motion of the gears' components.

The friction force calculated from the static friction torque, 1.4 Nm, and the diameter of the wheelchair wheel, 559.8 mm (22 inches), is about 10 N. In other words, the rider has to apply an extra 5 N to each wheel to overcome the friction force. The rolling resistance is usually assumed to be 1/100 of the normal force [27]. In this experiment, the mass of the rider and wheelchair was about 92 kg, and the rolling resistance was about 9 N ($\approx 92\ \text{kg} \times 9.8\ \text{m/s}^2 \times 0.01$). The sum of the rolling resistance and the friction force was 19 N, which was the minimum force required for the wheelchair to start to move. Additionally, 19 N is the parallel component to the force of gravity when a mass of 19 kg is on an inclined plane at angle of 6 degrees ($19\ \text{kg} \times 9.8\ \text{m/s}^2 \times \sin 6^\circ \approx 19$ N). This means that, due to the rolling resistance and the static friction of the driving mechanism, the wheelchair can stay stable on a hill when the mass error is less than 19 kg. If the angle of inclination decreases, the tolerance increases (tolerance mass = 19 N / ($9.8\ \text{m/s}^2 \times \sin\theta$)).

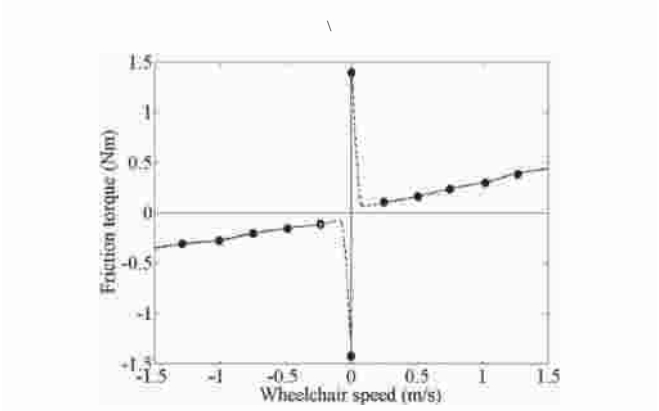

Fig. 11. Friction torque of driving mechanism.

Fig. 12. Experiment on a hill with gravity compensation.

B. Experiment With Gravity Compensation

To compensate for the force of gravity on a hill, the required current i is calculated from (1) and the relation between torque and current is shown in (13).

$$i = \frac{\tau}{K_t} \tag{16}$$

The calculated current, depending on the slope angle, is applied to each motor, and Fig. 12 shows that the wheelchair can compensate for the component of the gravity vector parallel to the inclined plane of 10 degrees. We also verified that the wheelchair can be maintained in a static condition at various angles of inclination.

C. Experiment for Friction Compensation

The friction in the driving mechanism is compensated for so that the rider is able to propel the wheelchair in the same way that he/she propels a manual wheelchair. The decelerating characteristic of a manual wheelchair is measured as reference data, and it is compared with that of the prototype.

To measure the decelerating characteristics, a wheelchair was dragged by an external driving mechanism. In this experiment, we used a 1.5 kW BLDC motor, reduction gear, pulley and rope. When the speed of the wheelchair reached a predetermined value, the external driving mechanism stopped pulling it. Then, the wheelchair decelerated and the wheelchair displacement was measured by integrating the incremental encoder pulses of the driving motor. The displacement of the manual wheelchair was measured by a laser distance sensor, because a manual wheelchair does not have an encoder.

Fig. 13 shows these results. The lines of the graph are not smooth, because the speeds are derived by differentiating the wheelchair displacement, but the overall decelerating rates are clearly shown. The speed of the prototype (red line with square) decreases faster than that of the manual wheelchair (black line with circle) due to the friction of the driving mechanism.

Fig. 14 shows the decelerating characteristic when a constant current is applied to the driving motor. In order to compensate for the frictional force accurately, the current would need to be changed, depending on the wheelchair speed (Fig. 11). However, in this research, applied currents are constants for simplicity and stable operation of the system, and to compensate

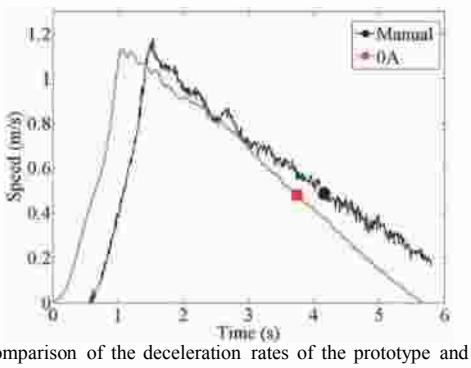

Fig. 13. Comparison of the deceleration rates of the prototype and a manual wheelchair.

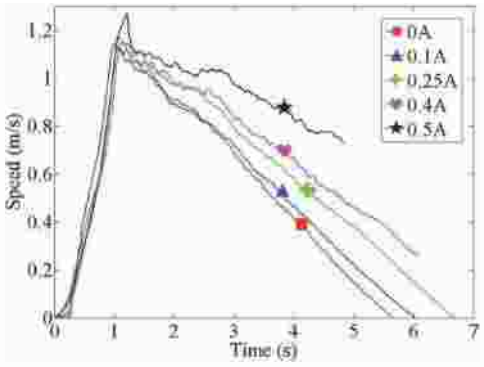

Fig. 14. Deceleration rates according to the current for friction compensation.

for the energy loss due to the large static friction (Fig. 4).

As the applied current increases, the deceleration rate decreases, and the prototype has a similar deceleration rate to the manual wheelchair at 0.25 A. Over the current, the additional current acts as if it were removing the other frictions, such as tire rolling resistance, so that the prototype moves further than the manual wheelchair with one instance of propulsion, such that the rider is able to move with less power being needed.

D. Experiment for Gravity and Friction Compensation

Compensation for gravity and friction simultaneously was performed. The wheelchair was dragged on a hill by an external driving mechanism as mentioned in section *C*. When the wheelchair speed reached a predetermined value, the external driving mechanism stopped pulling it. Then, the wheelchair decelerated and the displacement was measured. Fig. 15 shows the results. The red (square) line, dropping rapidly, is the speed of the prototype without any compensation. The green (cross) line, similar to the red line but dropping slightly slowly, is the speed of the prototype with only the frictional compensation. The blue (triangle) line, showing a big difference relative to the previous two lines, represents the speed of the prototype with gravity compensation. The pink (heart) line, dropping most slowly, represents the speed of the prototype with both the gravity and friction compensation.

The black (circle) line in Fig. 16 represents the speed of the manual wheelchair on a flat road (the same as the black (circle) line in Fig. 13) and the red (heart) line represents the speed of the prototype with gravity and friction compensation on a hill (the same as the pink (heart) line in Fig. 15). The maximum velocities at which the wheelchairs start to decelerate are different, due to the short distance of the inclined plane, but the deceleration rate is almost the same. That is to say, the rider on the prototype is able to climb the hill as if he or she were moving on a flat road.

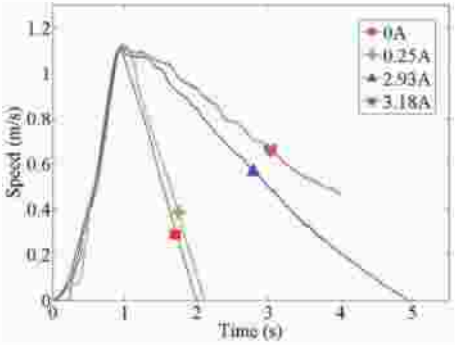

Fig. 15. Deceleration rate on an inclined plane with/without gravity and friction compensation.

To verify the practical performance of the GCPAW prototype, it was tested on a public road (Fig. 17). At first, it was used as a manual wheelchair on a flat road by disconnecting the clutch. Next, the clutch was connected and a friction-overcompensation current (current for friction compensation plus alpha) was applied. It was verified that the GCPAW went further with the same propulsion. In this friction-overcompensation mode, the power consumption was below 20 W, which is very low compared to the power consumption of conventional electric wheelchairs. When the GCPAW met a slope and the angle of tilt of the sensor exceeded the threshold, the GCPAW started automatically to compensate for the gravity component. The rider was able to climb a steep road, stop and make a delicate movement in the middle of the hill, just as if he or she were on a flat road. The rider could use his/her hands freely on the hill.

Fig. 18 shows the tilt sensor output and motor current when the wheelchair starts to move on flat land and then ascends a slope. The green (triangle) line shows the displacement of the wheelchair, which is the integrated value of the incremental

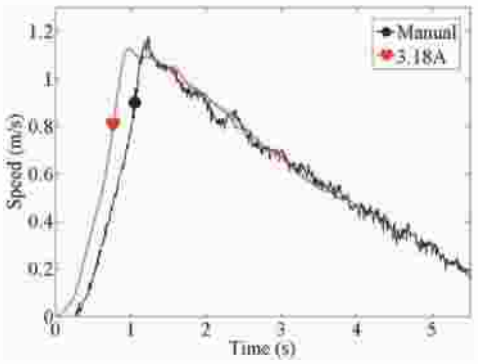

Fig. 16. Comparison of deceleration rates: Manual wheelchair on a flat road vs. the prototype with compensation on a hill.

Fig. 17. Performance test on a public road and on a slope at the entrance.

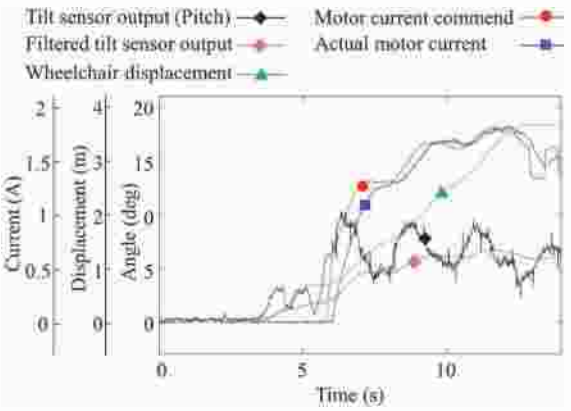

(a)

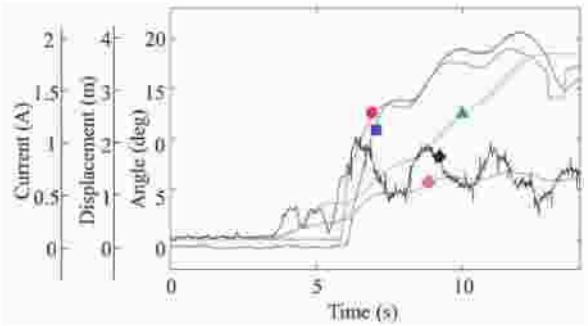

(b)

Fig. 18. Tilt sensor outputs and motor currents when the wheelchair starts to move on flat land and then ascends a slope. (a) Right wheel. (b) Left wheel.

encoder signal. In order that the tilt sensor is not affected by the acceleration or deceleration of the wheelchair, the raw data on the tilt sensor's output (the black diamond line) is filtered by the first-order infinite impulse response (IIR) filter with a sampling frequency of 100 Hz and a cutoff frequency of 0.1 Hz. When the filtered sensor signal (the pink cross line) reaches an angle of 2 degrees (around 6 s), the right and the left motors start to compensate for the gravity force. The red (circle) line represents the current command, and the blue (square) line represents the actual current of the motor. Fluctuations in the current command when the wheelchair is stopped (around 13 s) are caused by the friction compensation in the nonlinear model shown in Fig. 4. Although the raw data on the tilt sensor's output fluctuates because of the acceleration and deceleration of the wheelchair, by applying the low-pass filter algorithm, the wheelchair compensates for the gravity force in a stable manner.

E. Independent Wheel Torque Control

A generalized model was explained at the end of section II. A wheelchair sometimes moves obliquely up a slope. In this case, the wheelchair tilts slightly in the roll direction as well as in the pitch direction. In this case, the right and the left wheels should generate unequal torques. An experiment was performed to test the independent control of the wheel torques on a two-directional slope. It is not easy to make a precise and rigid slope similar to that shown in Fig. 5. Therefore, instead of manufacturing a two-directional slope, we performed the experiment on an ordinary one-directional slope (Fig. 2), which we had already used in the above experiments. By rotating the wheelchair by β on the slope (yaw motion, Fig. 19), the wheelchair becomes to be on a two-directional slope. The θ and ϕ shown in Fig. 5 can be derived from α and β. The results are provided in (17) and (18).

$$\sin\theta = \sin\alpha\cos\beta \tag{17}$$

$$\sin\phi = \sin\alpha\sin\beta \tag{18}$$

On the one-directional slope, the wheelchair with a rider is stopped, and the gravity compensated by (11) and (12). It is then rotated by about 30 deg, 60 deg, -30 deg, and -60 deg. The tilt sensor data and the motor current are then measured. Fig. 20 shows the results when α = 5.6 deg, w = 0.6 m, and d = 0.12 m.

The pink (cross) and black (diamond) lines show the filtered ϕ and θ angles, respectively. The blue (square) line shows the right motor current, and the red (circle) line shows the left motor current. The experimental results showed that the right and left wheel torques were independently controlled as the wheelchair rotated in a yaw axis on a slope.

The torque difference $\tau_R - \tau_L$ (= $\frac{\text{right motor current}}{\text{left motor current}}$) in (11) and (12) is about 10 N when α = 6˚and β = 15˚. The forces are smaller than the friction and rolling force mentioned in section IV-A. Therefore, in normal wheelchair usage, in which the wheelchair does not experience a large roll and pitch angle, it is not necessary to control the right and left wheel torques independently.

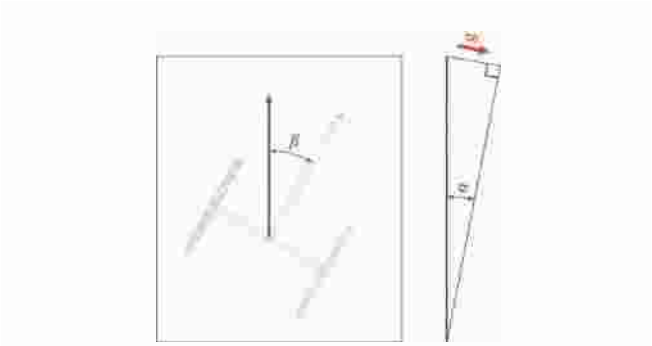

Fig. 19. Experiment on slanting slope.

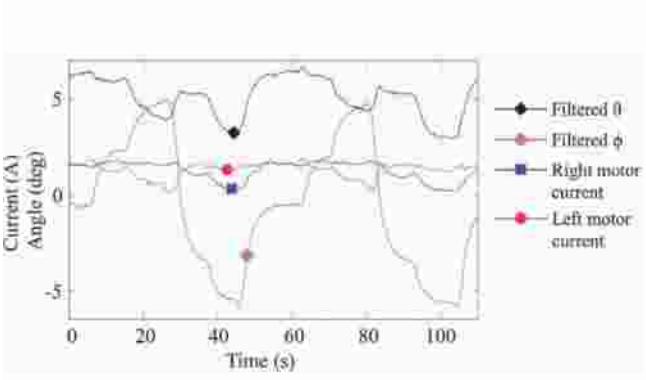

Fig. 20. Filtered tilt sensor outputs and right and left wheel torques during yaw motions on a slope.

V. Conclusion

A manual wheelchair is difficult to propel up a hill. In this research, we proposed a GCPAW that compensates for the force of gravity and the friction in the driving mechanism. The performance was verified through experimentation. The rider was able to climb a hill, stop and make a delicate movement in the middle of the hill, just as if he/she were on a flat road. The rider could use his/her hands freely on the hill.

It might be misconstrued that unless the assisting force for gravity compensation is exactly equal to the component of the gravity vector parallel to the inclined plane, the wheelchair will roll back down, or even up the hill. However, the friction in the driving mechanism and the rolling resistance of the tires absorb the error between the estimated value and the actual value of the parallel component to the force of gravity. That is to say that the friction forces prevent the wheelchair from either rolling back down or even up, despite some modelling errors.

Also, the overcompensation for the driving mechanism friction has the effect of reducing other frictions, such as the tire rolling friction, so that with the same propulsion the rider travels further than in a manual wheelchair. The wheelchair user travels longer distances per turn, and can reduce the arm effort needed.

References

[1] R. Lu, Z. Li, C.-Y. Su, and A. Xue, "Development and Learning Control of a Human Limb With a Rehabilitation Exoskeleton," *IEEE Trans. Ind. Electron.*, vol. 61, no. 7, pp. 3776-3785, Jul. 2014.

[2] J. Zhu, Q. Wang, and L. Wang, "On the Design of a Powered Transtibial Prosthesis With Stiffness Adaptable Ankle and Toe Joints," *IEEE Trans. Ind. Electron.*, vol. 61, no. 9, pp. 4797-4807, Sep. 2014.

[3] R. J. Farris, H. A. Quintero, S. A. Murray, K. H. Ha, C. Hartigan, and M. Goldfarb, "A Preliminary Assessment of Legged Mobility Provided by a Lower Limb Exoskeleton for Persons With Paraplegia," *IEEE Trans. Neural Syst. Rehabil. Eng.*, vol. 22, no. 3, pp. 482-490, May 2014.

[4] C.-H. Yu, Y.-J. Piao, K. Kim and T.-K. Kwon, "Characteristic Analysis of the Lower Limb Muscular Strength Training System applied with MR Dampers," *Biomed. Mater. Eng.*, vol. 24, no. 1, pp. 297-306, 2014.

[5] R. A. Cooper, R. Cooper, and M. L. Boninger, "Trends and Issues in Wheelchair Technologies," *Assist. Technol.*, vol. 20, no. 2, pp. 61-72, 2008.

[6] M. J. Wineman, "Design and Effects on Handrim Kinetics of an Automatic Gear-shifting Wheelchair For Manual Wheelchairs," M.S. dissertation, Dept. of Mechanical Engineering, Univ. of Illinois at Urbana-Champaign, 2014.

[7] Add on power unit, http://www.thebuzzycompany.com/features.html

[8] http://www.yankodesign.com/2012/01/27/independent-wheelchair-assistant/

[9] Hirokazu Seki, K. Ishihara, and S. Tadakuma, "Novel Regenerative Braking Control of Electric Power-Assisted Wheelchair for Safety Downhill Road Driving," *IEEE Trans. Ind. Electron.*, vol. 56, no. 5, pp. 1393-1400, May 2009.

[10] Yamaha wheelchair assist unit, http://www.yamaha-motor.co.jp/wheelchair/lineup/jwx2/ (in Japanese).

[11] E-motion wheelchair, http://www.frankmobility.com/e-motion.php

[12] Ottobock wheelchair, http://www.ottobock.com/cps/rde/xchg/ob_com_en/hs.xsl/3891.html

[13] Y. Heo, E.-P. Hong, and M.-S. Mun, "Development of power add on drive wheelchair and its evaluation," in *Proc. 9th Asian Control Conf. (ASCC) IEEE*, 2013, pp. 1-6.

[14] R. A. Cooper, T. A. Corfman, S. G. Fitzgerald, M. L. Boninger, D. M. Spaeth, W. Ammer, and J. Arva, "Performance assessment of a push-rim-activated power-assisted wheelchair control system," *IEEE Trans. Control Syst. Technol.*, vol. 10, no. 1, pp. 121-126, Jan. 2002.

[15] M. GM Kloosterman, G. J Snoek, L. HV van der Woude, J. H Buurke and J. S Rietman, "A system-atic review on the pros and cons of using a pushrim-activated power-assisted wheelchair," *Clin. Rehabil.*, vol. 27, no. 4, pp. 299-313, Mar. 2013.

[16] R. Simpson, E. LoPresti, S. Hayashi, S. Guo, R. Fisch, A. Martin, W. Ammer, D. Ding, and R. Cooper, "The Smart Power Assistance Module for Manual Wheelchairs," in *Proc. Technology and Disability: Research, Design, Practice and Policy, 26th Int. Annual Conf. on Assistive Technology for People with Disabilities (RESNA)*, 2003, pp. 51-54.

[17] S. Oh, N. Hata, and Y. Hori. "Integrated motion control of a wheelchair in the longitudinal, lateral, and pitch directions," *IEEE Trans. Ind. Electron.*, vol. 55, no. 4, pp. 1855-1862, Apr. 2008.

[18] S. Oh, and Y. Hori. "Disturbance attenuation control for power-assist wheelchair operation on slopes." *IEEE Trans. Control Systems Technology*, vol. 22, no.3, pp. 828-837, May 2014.

[19] J. Kim, S.-J. Lee, S. S. Lee, R. Sohn, and S. Lim, "Feasibility study on health monitoring intervention: Measuring body weight for wheelchair users," in *Proc. RESNA Int. Conf.*, 2011.

[20] K.-B. Jang and D.-W. Kang, "Development of a wheelchair based body weight scale for people with disabilities," in *Proc. 4th Int. Convention on Rehabilitation Engineerng & Assistive Technology*, 2010, Article No. 37.

[21] B. Armstrong and C.C. de Wit, "Friction Modeling and Compensation," *The Control Handbook, CRC Press*, 1995. http://www.mathworks.co.kr/kr/help/physmod/simscape/ref/translationalfriction.html.

[22] G. Cazzulani, C. Ghielmetti, H. Giberti, F. Resta and F. Ripamonti, "A test rig and numerical model for investigating truck mounted concrete pumps," *Automation in Construction*, vol. 20, no. 8, pp. 1133-1142, Dec. 2011.

[23] S. Oh, K. Kong, and Y. Hori, "Design and Analysis of Force-Sensor-Less Power-Assist Control," *IEEE Trans. Ind. Electron.*, vol. 61, no. 2, pp. 985-993, Feb. 2014.

[24] T. Shibata and T. Murakami, "Power-Assist Control of Pushing Task by Repulsive Compliance Control in Electric Wheelchair," *IEEE Trans. Ind. Electron.*, vol. 59, no. 1, pp. 511-520, Jan. 2012.

[25] Y. Oonishi, S. Oh, and Y. Hori, "A New Control Method for Power-Assisted Wheelchair Based on the Surface Myoelectric Signal," *IEEE Trans. Ind. Electron.*, vol. 57, no. 9, pp. 3191-3196, Sep. 2010.

[24] S.-W. Hwang, C.-H. Lee and Y.-B. Bang, "Power-Assisted Wheelchair with Gravity Compensation," in *Proc. 12th Int. Conf. on Control, Automation and Systems*, 2011, pp. 1874-1877.

[25] A. M. Kwarciak, M. Yarossi, A. Ramanujam, T. A. Dyson-Hudson, and S. A. Sisto, "Evaluation of wheelchair tire rolling resistance using dynamometer-based coast-down tests," *J. Rehabil. Res. Dev.*, vol. 46, no. 7, pp. 931-938, 2009.

Kyung-min Lee received the B.S. and Ph.D. degrees in Mechanical and Aerospace Engineering from Seoul National University, Seoul, Korea, in 2000 and 2006, respectively. He carried out research at SNU and the University of Toronto as a post-doctoral fellow and at Hyundai Motors Company R&D division as a senior research engineer. He is currently a patent examiner in Korean Intellectual Property Office, Daejeon, Korea. His research field includes design, modelling, and simulation of robot and mechatronic system.

Chang-Hyuk Lee received the B.S. degree in biological industry and mechanical engineering from Konkuk University, Chungju, Korea, in 2009. Since September 2009, he has been working toward the Ph.D. degree at the Department of Transdisciplinary Studies, Seoul National University, Suwon, Korea. His research interests include electromagnetic system design, assistive technology, and exoskeletal robotic systems.

Soonwook Hwang received the B.S. degree in mechanical and aerospace engineering from Seoul National University, Seoul, Korea. He is currently a Ph.D candidate in the Graduated School of Convergence Science and Technology at Seoul National University, Suwon, Korea. His research interests include whole-body control framework, multicontact control, legged locomotion, compliant control, and design & manufacturing of robots.

Jiwon Choi received the B.S. degree in electrical engineering from Ajou University, Suwon, Korea, in 2013. He received the M.S. degree in convergence science and technology from Seoul National University, Suwon, Korea, in 2015. He was with Kyungwoo Systech Inc. from 2007 to 2010. Since 2015, he has been with the University of Texas Health Science Center at Houston. His research interests include smart actuator system and its biomedical applications.

Young-bong Bang (M'03) received the B.S. and M.S. degrees in mechanical engineering from Seoul National University, Seoul, Korea, in 1989 and 1991, respectively, and the Ph.D. degree in precision machinery engineering from The University of Tokyo, Tokyo, Japan, in 1997. From 1997 to 1999, he was with FANUC Ltd. From 2000 to 2009, he was with the School of Mechanical and Aerospace Engineering, Seoul National University, Seoul, Korea. Since 2009, he has been with the Advanced Institutes of Convergence Technology, Seoul National University, Suwon, Korea. His research interests include actuator-based mechatronic systems, personal mobility, and assistive technology.